Desalination and Water Treatment
www.deswater.com
doi: 10.1080/19443994.2015.1112309

57 (2016) 20714–20725
September

Taylor & Francis
Taylor & Francis Group

Adsorption characteristics of 4-hydroxy-3-aminophenylarsonic acid (HAPA) onto anaerobic granular sludge

Jun-Chao Li[a], Shou-Jun Yuan[a,c], Wei Wang[a,c], Feng Ji[b], Zhen-Hu Hu[a,c,*]

[a]*School of Civil Engineering, Hefei University of Technology, Hefei 230009, China, Tel. +86 551 62904144; email: 794129072@qq.com (J.-C. Li), Tel. +86 551 62904148; emails: sjyuan@hfut.edu.cn (S.-J. Yuan), dwhit@163.com (W. Wang), zhhu@hfut.edu.cn (Z.-H. Hu)*

[b]*Institute of Animal Husbandry and Veterinary Medicine, Beijing Academy of Agriculture and Forestry Sciences, Beijing 100097, China, Tel. +86 10 51503301; email: fengjp3@hotmail.com*

[c]*Institute of Water Treatment and Wastes Reutilization, School of Civil Engineering, Hefei University of Technology, Hefei 230009, China*

Received 19 March 2015; Accepted 18 October 2015

ABSTRACT

Four-hydroxy-3-aminophenylarsonic acid (HAPA) is the degradation product of 3-nitro-4-hydroxyphenylarsonic acid (roxarsone, a widely used organoarsenic additive in animal feed) under anaerobic conditions. HAPA is highly water soluble and resistant to degradation by anaerobic micro-organisms. In this study, the effect of initial concentration, temperature, pH, ionic strength, and interferential ions on the adsorption of HAPA onto anaerobic granular sludge (AGS) was investigated using batch adsorption experiments. The results showed that equilibrium state of the adsorption was reached at about 10 h. The kinetics analysis indicated that the adsorption process followed a pseudo-second-order model and intra-particle diffusion was the rate-limiting step. The adsorption mechanisms could be explained by the Freundlich and D–R isotherm models. The maximum adsorption capacity of HAPA onto AGS was 12.57, 25.05, and 26.31 mg/g at 15, 25, and 35°C, respectively. pH, ionic strength, and phosphate ions had obvious negative effect on the HAPA adsorption onto AGS. Thermodynamics analysis confirmed that the adsorption of HAPA onto AGS was an endothermic and spontaneous process. The results obtained from this study will improve the understanding to the adsorption characteristics of HAPA onto AGS and the fate of roxarsone in anaerobic sludge reactor.

Keywords: 4-hydroxy-3-aminophenylarsonic acid (HAPA); Anaerobic granular sludge (AGS); Adsorption; Kinetics analysis; Roxarsone

1. Introduction

Antibiotics have been widely used in animal husbandry for animal therapy and health protection since last century [1]. Roxarsone (3-nitro-4-hydroxyphenylarsonic acid) is an organoarsenic antibiotic and has been widely used to prevent coccidiosis and to stimulate growth as a feed additive in broiler and swine industries [2,3]. The permitted dose of roxarsone in the feed is in the range of 25–50 mg/kg, and high concentrations of arsenic from 0.4 to 119 mg/kg have been reported in the animal litters, supplementing

*Corresponding author.

organoarsenic additives [4]. Roxarsone has been banned to use in the Europe and USA in recent years but still can be used in many developing countries [4]. Most of the added roxarsone was excreted into manure and wastewaters with feces and was rapidly transformed into 4-hydroxy-3-aminophenylarsonic acid (HAPA) under anaerobic or anoxic conditions [5–8]. HAPA has been detected in fresh poultry litter [7], accounting for 12–25% of the identified arsenic species [9]. The molecular structures of roxarsone and HAPA are shown in Fig. 1.

HAPA is water soluble and resistant to be degraded by anaerobic micro-organisms [10]. It has been reported that HAPA was completely degraded over a 229-d incubation under anaerobic conditions [5], and even under electrical stimulation conditions, the complete degradation still needed one week [10]. In an anaerobic system, HAPA inhibited the activities of both acetoclastic and hydrogenotrophic methanogens at a concentration of 1 mmol/L and the inhibition increased sharply with the prolonging of the incubation time [8]. The structure of anaerobic granular sludge (AGS) was also affected by HAPA in the solution under anaerobic conditions, although only a small part of HAPA was fixed in the AGS [11].

Previous studies have investigated the influence of management methods on the fate and transformation of residual antibiotics in animal manures [12]. Anaerobic digestion was often applied to treat wastewaters from animal husbandry containing high concentration of organic matter using upflow anaerobic sludge blanket (UASB) bioreactor for recovering biogas as energy [13–15]. AGS is an aggregate of millions of micro-organisms with various species in the UASB reactor [16]. It has many characteristics, such as good microbial activities, excellent settling ability, and strong, compact and porous structure [17]. The adsorption of micro-contaminants such as tetracyclines [18], heavy metals onto AGS has been investigated in recent years [19].

However, there is little information regarding the adsorption process of HAPA onto AGS, which limits the understanding of HAPA behavior in the UASB reactor. Therefore, the objective of this study was to evaluate the sorption capacity of AGS onto HAPA and the kinetics of the sorption process, which will provide useful information for the management and operation of UASB reactor treating HAPA contaminated animal wastewater.

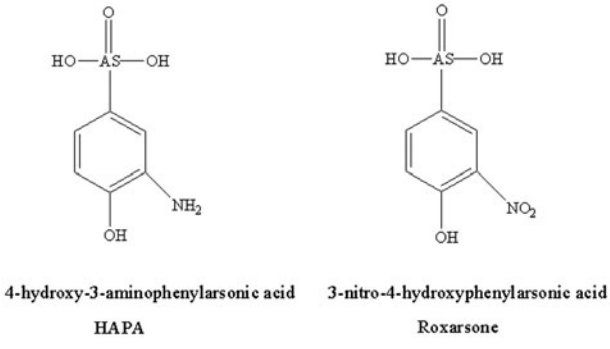

Fig. 1. Chemical structures of HAPA and roxarsone.

2. Materials and methods

2.1. Chemicals and anaerobic granule sludge

HAPA (purity > 97%) was purchased from Sigma Co. Ltd, China. All chemicals were reagent grade and used without further purification. Stock solution of HAPA was prepared with deionized water.

AGS used in this study was collected from a 10-L UASB reactor treating synthetic wastewater at 35 ± 2°C in the laboratory, then stored in a refrigerator at 4°C to avoid undesired metabolism. The moisture content of the AGS was 86.9% and volatile organic solid took up a proportion of 51.0% among the solid. The characteristics of the AGS are listed in Table 1.

2.2. Batch adsorption experiments

Batch adsorption tests were carried out in 150-mL flasks with a working volume of 100 mL. AGS and deionized water were firstly loaded into flasks, and then the flasks were flushed with nitrogen gas for 3 min to create anaerobic conditions and sealed with rubber stopper. At the beginning of the adsorption experiment, the determined volume of HAPA stock

Table 1
Characteristics of the anaerobic granule sludge

Items	Contents (%)
Moisture	86.94
VS	6.67
Ca	11.1427
P	6.4050
Zn	0.0812
Cu	0.0098
Ni	0.0413
Cr	0.0318
Mg	0.2755

Notes: The content of metals is based on the dry matter of the anaerobic granule sludge; VS, volatile solid.

solution was injected into the flasks based on the designed initial HAPA concentration. All flasks were placed in an air-bath shaker and operated at 150 rpm. The supernatant was regularly collected with syringes and filtered through a 0.22-μm cellulose acetate membrane for the determination of HAPA. All tests were performed in triplicate.

The AGS used per flask was 4.8 g (about 0.6 g of dry matter) for all tests, and the pH was adjusted around 7.0 ± 0.2 with 1.0 mol/L NaOH or HCl. In the test of contact time and initial concentration, the initial HAPA concentration was set at 2.0, 5.0, 10.0, and 20.0 mg/L, and the temperature was controlled at 25˚C. In the investigation of temperature, 15, 25, and 35˚C were selected and the initial HAPA concentration was 5.0 mg/L. In the analysis of adsorption equilibrium isotherm, the initial HAPA concentrations were set at 5.0, 10.0, 20.0, 50.0, and 100.0 mg/L with temperatures of 15, 25, and 35˚C, respectively. In the test of pH, the pHs of 5.0, 6.0, 7.0, 8.0, and 9.0 were investigated at 10.0 mg/L HAPA and 25˚C. For investigating the effect of ionic strength, NaCl concentrations of 10.0, 20.0, 30.0, 40.0, and 50.0 mg/L were used at 5.0 mg/L HAPA and 25˚C. In addition to investigate the effect of phosphorus ions on the adsorption, different concentrations of KH_2PO_4 (0.14, 0.68, and 1.36 g/L) were added into the system at 5.0 mg/L HAPA and 25˚C. The kinetics study for HAPA adsorption onto AGS was carried out at four different initial HAPA concentrations (2.0, 5.0, 10.0, and 20.0 mg/L) and 25˚C.

The amount of HAPA adsorbed by AGS was calculated as follows:

$$q_t = \frac{(C_0 - C_t)V}{W} \quad (1)$$

in which q_t is the amount of adsorbed HAPA per gram AGS at time t (mg/g), C_0 and C_t are the initial and residual concentrations of HAPA solution at time t (mg/L), respectively, V is the solution volume (L), W is the dry weight of AGS in the tests.

2.3. Desorption experiment

Batch desorption tests were conducted in duplicate to identify the reversibility of HAPA adsorption onto AGS. Adsorption experiment with initial 5.0 mg/L HAPA solution at 25˚C was operated at equilibrium state, and then the liquids were removed. The left saturated granules (about 4.8 g) in the flask were transferred to a column system for desorption test. The column system was composed of a plastic column which was 110 mm in height and 30 mm in inner diameter and a peristaltic pump was used to feed deionized water from the bottom of the column. The flow rate was controlled at 4.8 mL/min with liquid retention time of approximately 15 min. The effluent was collected and filtered for the determination of HAPA.

2.4. Analytical methods

HAPA concentration was determined by a high-performance liquid chromatography (HPLC, Shimadzu LC-20AD, Japan) equipped with a UV detector (SPD-20A). The wavelength of the UV detector was set at 264 nm. A Wondasil C18 column (4.6 mm × 150 mm, 5 μm, GL Sciences Inc.) was used for the separation of HAPA. The mobile phase was composed of 0.05 M KH_2PO_4, methanol, and formic acid (90:10:0.1, V/V/V) at a flow rate of 1.0 mL/min and the column temperature was controlled at 30 ± 1˚C.

The concentration of inorganic arsenic was measured using atomic fluorescence spectrometry (AFS-8220, Titan Beijing, China). Argon gas was used as carrier gas. Deionized water mixed with 2% potassium borohydride (KBH_4, W/V) and 0.5% potassium hydroxide (KOH, W/V) was provided as a reducing agent. Solution of 7% HCl (V/V) was used as current-carrying liquid. Surface morphology of AGS was investigated using scanning electron microscopy (SEM). The functional groups on AGS surface before and after adsorption were characterized by Fourier transform infrared spectrum (FTIR, Nicolete 10, Thermo Fisher, USA). Surface area was calculated based on N_2 Brunauer–Emmett–Teller (BET) analysis (Tristar II 3020, USA).

3. Results and discussion

3.1. Characterization of AGS

Surface area of AGS was determined by BET analysis with 7.139 m^2/g. The SEM micrograph of AGS is shown in Fig. 2. No apparent cracks were found on the surface of AGS, indicating the steady structure and good stability. The FTIR analysis is shown in Fig. 3 with a number of peaks. The broad and strong bands around 3,435 cm^{-1} were due to the overlapping of OH and NH stretching [20]. The band around 2,925 cm^{-1} showed the C–H stretching vibrations of $–CH_3$ and $>CH_2$ functional groups [21]. The band around 1,652 cm^{-1} corresponded to the C=O stretch. The peak around 1,056 cm^{-1} was related to the −OH stretching

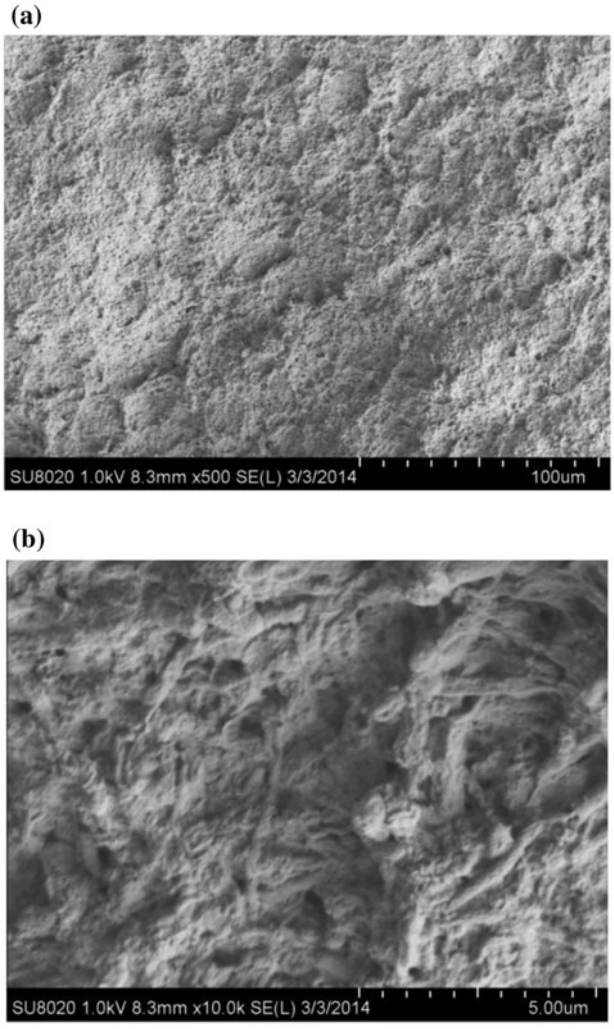

Fig. 2. SEM micrograph of AGS (magnification: (a) 500 and (b) 10,000).

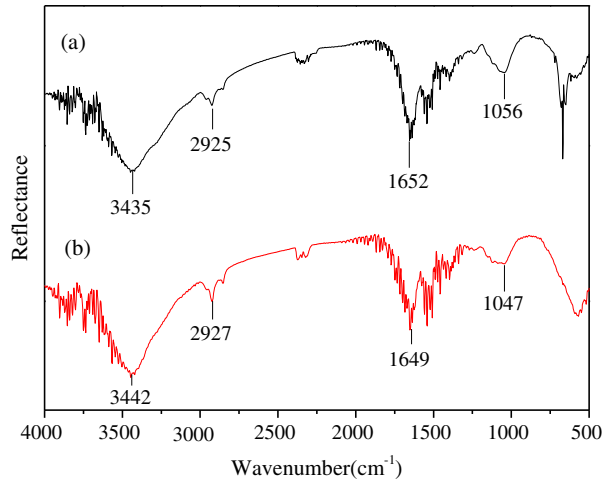

Fig. 3. FTIR spectra of AGS: (a) before adsorption and (b) after adsorption.

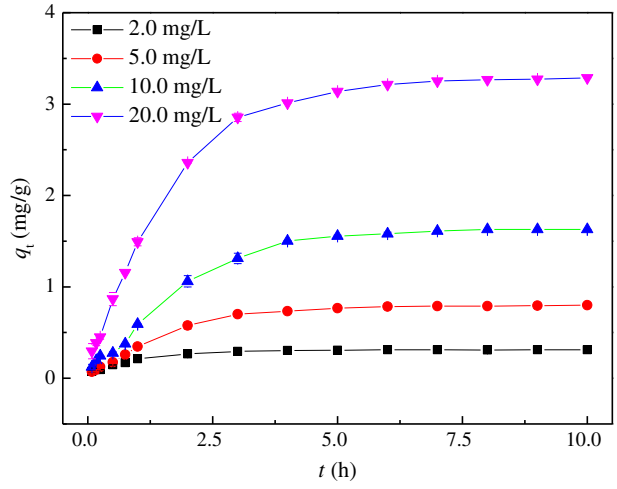

Fig. 4. Effect of contact time and initial concentration on the adsorption at 25°C.

vibrations [22]. The peaks between 1,056 and 1,652 cm^{-1} were probably related to S=O stretching [23]. According to the comparison of the peaks before and after adsorption, there were no significant changes in the functional groups mentioned above in the adsorption process.

3.2. Effect of environmental factors

3.2.1. Effect of contact time and initial concentration

In the control test without AGS addition, the result showed that the adsorption of HAPA onto container walls could be neglected. Fig. 4 shows the effect of contact time and initial concentration on the adsorption of HAPA onto AGS at 25°C. It was found that the amount of HAPA absorbed increased with the increase in contact time. Similar trend was also found in the adsorption of arsenate onto the anaerobic biomass [24]. A rapid adsorption process occurred in the first 3 h, and more than 60% HAPA was absorbed during this stage. After then, the adsorption rate gradually decreased until reaching equilibrium state at about 10 h. The fast adsorption of HAPA onto AGS in the initial stage was contributed to the availability of uncovered surface and activated sites on the surface of AGS [25]. The adsorption of HAPA was also dependent on the initial HAPA concentration. When the initial HAPA concentration increased from 2.0 to 20.0 mg/L, the amount of absorbed HAPA increased from 0.31 to 3.29 mg/g at equilibrium time. This could

be explained that, with the increase in the initial concentration, driving force was increased to overcome the resistance of mass transfer between the aqueous and solid phases [22,26], which leads to more active sites being occupied by HAPA on the surface of AGS.

3.2.2. Effect of pH and ionic strength

pH is one of the main factors that affect the adsorption process [17,27]. The effect of initial pH on the adsorption was shown in Fig. 5(a). When the initial pH increased from 5.0 to 9.0, the equilibrium uptake decreased from 1.70 to 1.45 mg/g. Similar trend was reported in the biosorption of Direct Black 38 [28] and chlorophenols [29] by AGS. It has been reported that when pH is above 3, the overall surface charge on the cells become negative [29,30]. The pK_{a1} value of HAPA is under 5.0 [4]. When pH is higher than 5, negatively charged ionized form of HAPA dominates in the solution. As the solution pH increased from 5.0 to 9.0, the adsorption between negatively charged HAPA and binding sites of the biomass surface decreased. Meanwhile, the presence of OH^- ions under alkaline conditions also affects the adsorption of HAPA [28], because of OH^- ions competing with adsorption sites with negatively charged HAPA, which also resulted in the decrease in equilibrium uptake.

The influence of ionic strength on the adsorption of HAPA onto AGS is shown in Fig. 5(b). The equilibrium uptake decreased from 0.79 to 0.65 mg/L with the increase in ionic strength from 0 to 50 mg/L NaCl, indicating that ionic strength has negative effects on the adsorption. Similar result has been reported in the adsorption of roxarsone by multi-walled carbon nanotubes [31].

3.2.3. Effect of phosphate

Phosphate is one of the most ubiquitous aqueous anions in aquatic environment. On account of the chemical similarities between phosphorus and arsenic, the competitive adsorption to active sites always occurs on surfaces [32–34]. Thus, it is of considerable interest to study the influence of phosphate on the adsorption of inorganic arsenic compounds [34,35], but the effect of phosphate on organic arsenic compounds is still unknown. Fig. 6 shows that the presence of phosphate had an obvious adverse effect on the process of adsorption. The adsorption capacity of AGS toward HAPA decreased with the increase in phosphate concentration in the bulk solution. According to the experimental

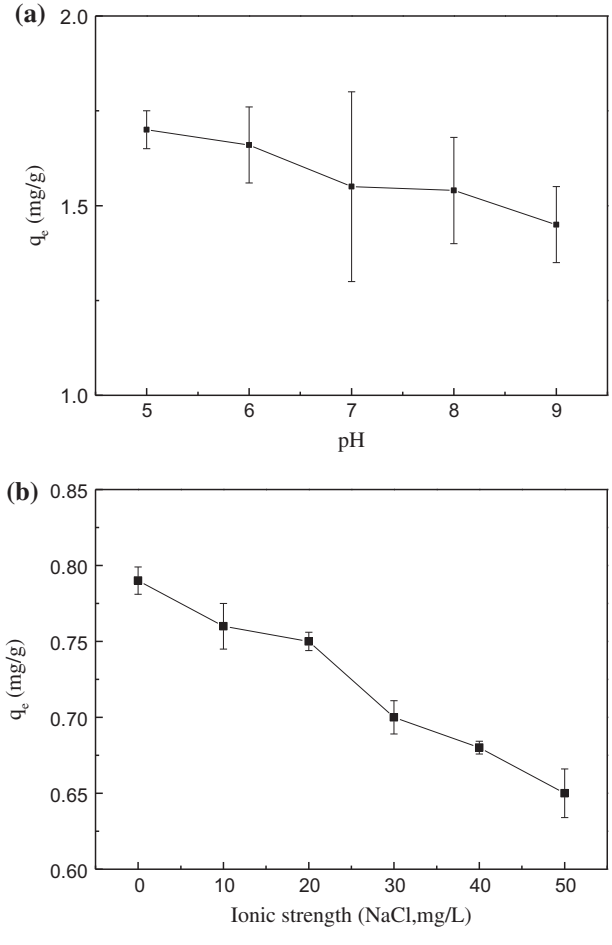

Fig. 5. Effect of pH and ionic strength on the adsorption at 25℃: (a) 10.0 mg/L HAPA and (b) 5.0 mg/L HAPA at pH 7.

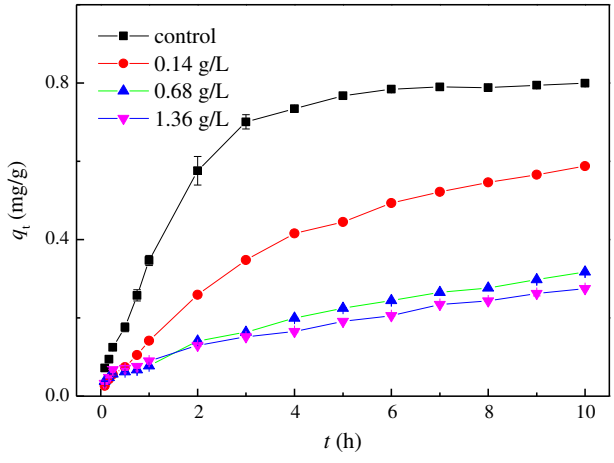

Fig. 6. Effect of phosphate on the adsorption at initial 5.0 mg/L HAPA at 25℃.

data, 50, 77, and 78% of HAPA was inhibited by KH_2PO_4 solution at 0.14, 0.68, and 1.36 g/L in the initial 3 h, indicating that phosphate competes with HAPA for the active sites. Therefore, phosphate in the solution has negative influence on the adsorption of HAPA onto AGS in UASB system.

3.3. Adsorption kinetics

Adsorption kinetics describes the solute uptake rate at the solid–aqueous interface, which provides evident information about the rate-controlling step and the possible mechanisms of the adsorption [36]. The pseudo-first-order, pseudo-second-order, and intra-particle diffusion models were applied to analyze the adsorption kinetics in this study. Correlation coefficient (R^2) was calculated to evaluate the conformity between experimental data and the model predicted values. Generally, high R^2 values indicate that the adsorption processes are well described by the kinetics models.

The pseudo-first-order equation is expressed as the following:

$$\log(q_e - q_t) = \log q_e - \frac{K_1 t}{2.303} \quad (2)$$

in which q_e and q_t are the amounts of adsorbed HAPA per gram AGS at equilibrium time and time t (mg/g), respectively, and K_1 (min^{-1}) is rate constant of the first-order adsorption.

The linear fitting form of pseudo-first-order kinetic model for the adsorption of HAPA onto AGS is exhibited in Fig. 7. The curves were linear in the first 6 h, with correlation coefficient (R^2) over 0.990. However, the pseudo-first-order kinetic model had a low correlation coefficient to fit the whole adsorption process, showing the bad quality of linearization. Thus, the whole adsorption process couldn't be described by pseudo-first-order kinetic model, indicating that pseudo-first-order kinetic model cannot explain the adsorption mechanism of HAPA onto AGS. Therefore, pseudo-second-order equation was tried to fit the experimental data.

The pseudo-second-order equation is described as:

$$\frac{t}{q_t} = \frac{1}{K_2 q_e^2} + \frac{t}{q_e} \quad (3)$$

in which q_e and q_t have the same meaning as in Eq. (2), K_2 is the rate constant (g/(mg min)). The value of K_2 was calculated from the intercept and the slope of the linear plot of t/q_t vs. t in Eq. (3).

The plot of t/q_t vs. t is shown in Fig. 8. The q_e and K_2 were calculated by the slopes and intercepts of the lines and are listed in Table 2. The values of R^2 for pseudo-second-order equation were greater than 0.989 at all concentrations, and the values of q_e were very close to the experimental data, indicating that pseudo-second-order kinetics fitted the adsorption process very well. A similar result was found on the hemicellulose-based absorbent toward dye [37]. A phenomenon should be pointed out that a little simulation deviation from the experimental data was found in the initial 1 h of the adsorption process (as shown in Fig. 4). It might be mainly caused by the complex components of AGS's surface, especially the

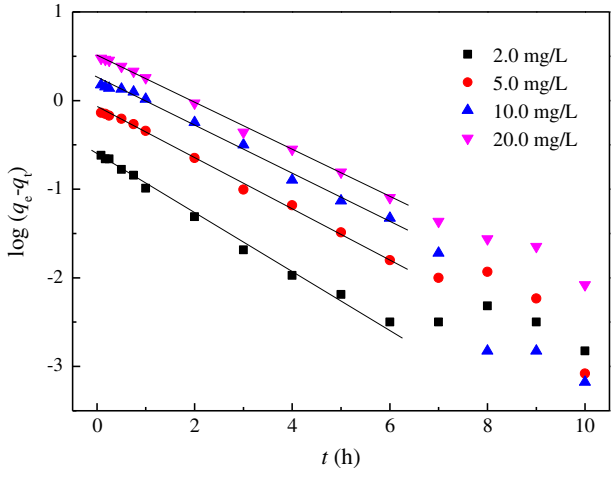

Fig. 7. Pseudo-first-order plot for HAPA adsorption onto AGS at different initial HAPA concentrations and 25℃.

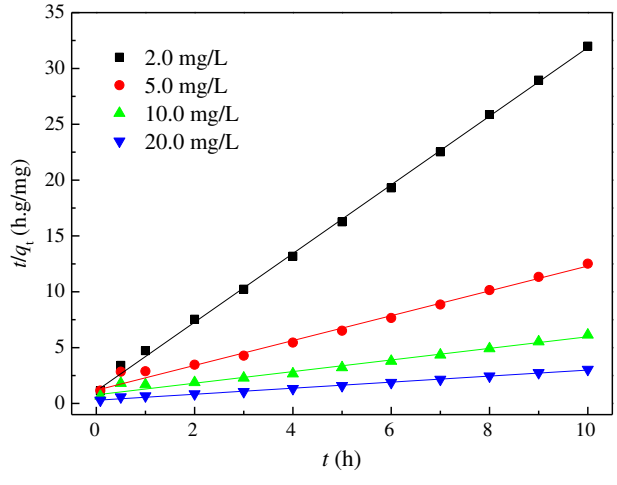

Fig. 8. Pseudo-second-order plot for HAPA adsorption onto AGS at different initial HAPA concentrations and 25℃.

Table 2
Kinetic parameters for the adsorption data at different initial concentrations

	Pseudo-first-order			Pseudo-second-order			
C_0 (mg/L)	K_1 (10^{-3}) min^{-1}	q_e (mg/g)	R^2	K_2 (g/(mg min))	q_e (mg/g)	$K_2q_e^2$ (mg/g min)	R^2
2.0	8.636	0.169	0.929	0.140	0.325	0.015	0.999
5.0	10.17	0.783	0.975	0.018	0.899	0.014	0.995
10.0	13.01	2.265	0.967	0.006	1.921	0.022	0.989
20.0	9.788	3.097	0.996	0.004	3.693	0.059	0.998

extracellular polymeric substances (EPS) [38]. It has been reported that the equilibrium time of toluidine blue adsorption onto EPS was about 90 min [39], and the EPS was considered as the main influence factor at the beginning of the adsorption process [40].

A multistep process always takes place during the adsorption, including surface diffusion, intra-particle or pore diffusion, and adsorption on the interior active sites [41], which can be analyzed through intra-particle diffusion model. The equation is expressed as:

$$q_t = k_i t^{\frac{1}{2}} + C \tag{4}$$

where k_i is the rate constant of the intra-particle diffusion (mg/g $min^{1/2}$), C is intercept (mg/g).

Fig. 9 shows the plot of q_t vs. $t^{1/2}$ for the adsorption of HAPA onto AGS. Based on the multilinearity simulation, the adsorption process could be divided into three portions, 0–3 h, 3–5 h, and 5–10 h. Based on the theory of adsorption multistep process, the first portion was attributed to the diffusion of HAPA molecules through the solution to the surface of AGS, the second portion was the gradual adsorption stage, in which intra-particle diffusion occurred, and the third portion approached equilibrium state, in which intra-particle diffusion started to slow down [42]. The slope of the second linear portion was obviously smaller than the first one, indicating that intra-particle diffusion portion was the rate-controlling step. The calculated values of k_i were given as 0.179, 0.393, 0.487, and 0.543 mg/g $min^{0.5}$, respectively. The corresponding values of C in the second portion, which was proportional to the boundary layer thickness [43], were 0.018, 0.020, 0.485, and 1.923 mg/g $min^{0.5}$ for the corresponding HAPA concentrations of 2.0, 5.0, 10.0, and 20.0 mg/L. These results indicated that high concentration of HAPA solution would lead to an increase in rate of intra-particle diffusion and more HAPA molecules into deeper interior for active adsorption sites.

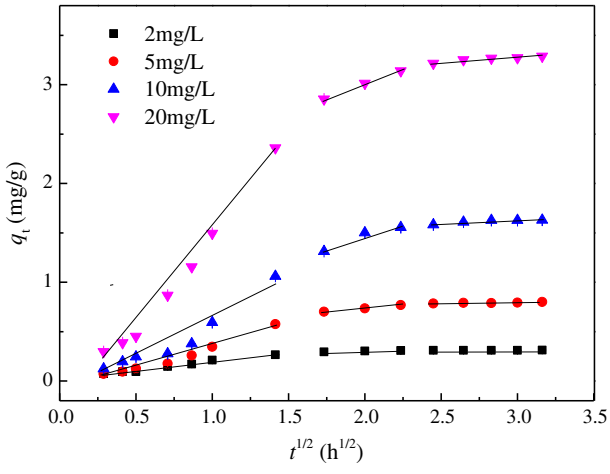

Fig. 9. Intra-particle diffusion plot for HAPA adsorption onto AGS at 25°C.

3.4. Equilibrium isotherms

Adsorption equilibrium isotherms provide fundamental physicochemical data for evaluating the applicability of adsorption process [44]. Three typical adsorption models, the Langmuir, the Freundlich, and the Dubinin–Radushkevich (D–R) [45] isotherms, were employed to describe the HAPA adsorption onto AGS in this study.

The Langmuir isotherm assumes that the solid has limited adsorption ability. All the adsorption sites are assumed to be identically, energetically, and sterically independent of the adsorbed quantity [46]. The surface reaches the saturation point when adsorption sites are completely occupied by the adsorbate molecules, and the maximum adsorption capacity will be achieved. The linear form of the Langmuir isotherm model is given as:

$$\frac{1}{q_e} = \frac{1}{k_L Q_{max} C_e} + \frac{1}{Q_{max}} \tag{5}$$

where Q_{max} (mg/g) is the theoretical maximum adsorption capacity of HAPA adsorbed by AGS, k_L (L/mg) is the constant of Langmuir isotherm related

to the energy or net enthalpy of adsorption, C_e (mg/L), the concentration of HAPA in the solution at equilibrium time.

The experimental data of 5.0 mg/L HAPA soluion at 15, 25, and 35℃ were plotted as $1/q_e$ against $1/C_e$ with the Langmuir isotherm in Fig. 10(a). The values of R^2 were 0.895, 0.905, and 0.980 at 15, 25, and 35℃, respectively, indicating poor correlation between the model and data, showing that the surface of AGS was not homogenous.

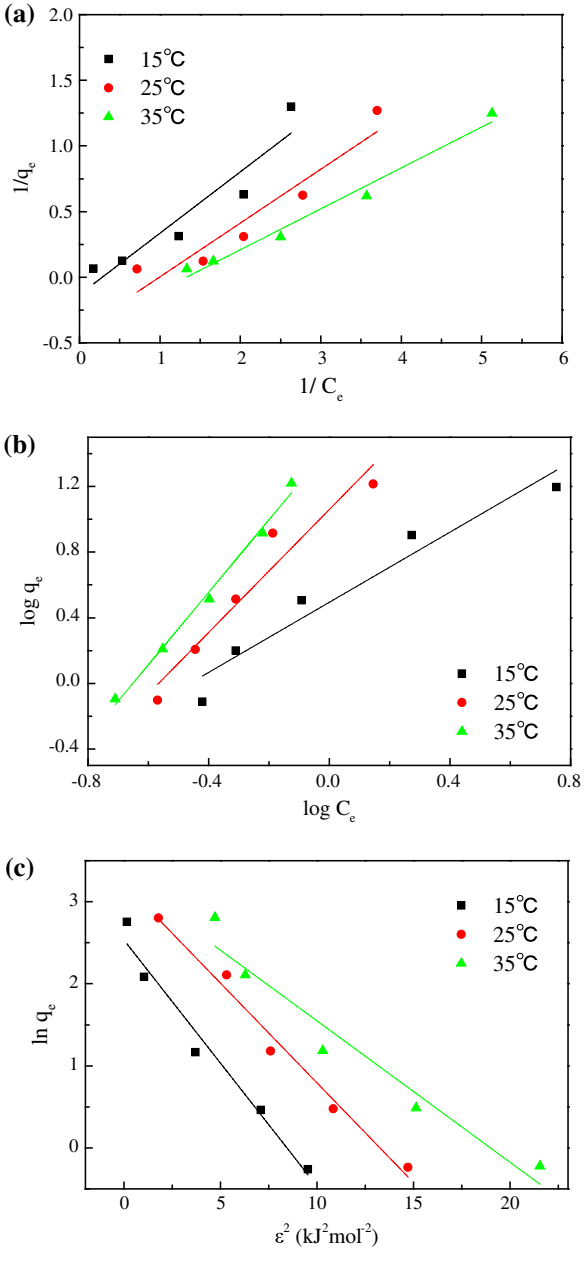

Fig. 10. Langmuir (a), Freundlich (b), and D–R (c) isotherms for the adsorption of HAPA onto AGS at different temperatures.

The Freundlich model is commonly used to describe the adsorption process onto heterogeneous surface of the adsorbent. The isotherm doesn't imply a saturation of the adsorptive surface. The Freundlich isotherm equation is given as:

$$\log q_e = \frac{1}{n} \log C_e + \log K_F \tag{6}$$

in which K_F and n are the Freundlich constants accounting for the adsorption capacity and intensity, respectively.

From Eq. (6), the value of K_F and n can be calculated from the intercepts and slopes of the fitting lines. If n value is close to one, it indicated that the adsorption is independent of the adsorbate concentration. Additionally, n value less than one indicated the adsorption is favored at a higher concentration [47]. As depicted in Fig. 10(b), the experimental data were plotted as $\log q_e$ against $\log C_e$ with the Freundlich model. The relative parameters are listed in Table 3, indicating that the Freundlich isotherm equation fitted the data well, which is similar to the result of 2,4-DCP adsorption onto AGS [29]. The values of K_F increased with the increasing temperature, showing that the adsorption capacity of AGS toward HAPA increased with the increasing temperature and the adsorption process was considered to be endothermic. All the values of n were under one, indicating the low adsorption intensity at a lower concentration. Therefore, the adsorption was favored at a higher concentration because of the increasing electrostatic attraction and driving force.

The D–R model was used to distinguish the type of physic-sorption or chemisorption and to assess the adsorption mechanism as well [48]. The Dubinin–Radushkevich (D–R) isotherm is given as:

$$\ln q_e = \ln Q_{max} - \beta\varepsilon^2 \tag{7}$$

$$\varepsilon = RT \ln(1 + 1/C_e) \tag{8}$$

$$E = \frac{1}{(2\beta)^{\frac{1}{2}}} \tag{9}$$

in which β is a constant related to the mean free energy (mol^2/kJ^2), ε is the Polanyi potential, R is the ideal gas constant (8.314 J/(mol K)), and E is mean free energy (kJ/mol).

The experimental data were plotted as $\ln q_e$ against ε^2 with the D–R model, as shown in Fig. 10(c). The

Table 3
Isotherm constants for adsorption of HAPA onto AGS

	Langmuir				Freundlich		D–R		
T (K)	Q_{max} (mg/g)	k_L (L/mg)	R^2	K_F	n	R^2	Q_{max} (mg/g)	β (mol^2/kJ^2)	R^2
288	−7.576	−0.283	0.895	3.119	0.936	0.936	12.57	0.300	0.971
298	−2.457	−0.993	0.905	11.46	0.534	0.940	25.05	0.243	0.983
308	−2.421	−1.328	0.980	27.42	0.453	0.993	26.31	0.172	0.948

values of Q_{max} and β were calculated by the intercepts and slopes of the fitting lines and are listed in Table 3. The values of R^2 showed a good conformity between the predicted values and data. The values of Q_{max} increased with the increasing temperature also indicating that the adsorption was an endothermic process. According to Eq. (9), E values were calculated, which were 1.29, 1.43, and 1.71 kJ/mol at 15, 25, and 35°C, respectively. As reported previously, when $E < 8$ kJ/mol, the adsorption process was considered to be a physical process [20,43]. Therefore, based on the results of the D–R model, the adsorption was considered to be mainly a physical process.

3.5. Thermodynamics analysis

Thermodynamics analysis is helpful to estimate the thermodynamic characteristics. The adsorption thermodynamics of HAPA onto AGS was analyzed at 288, 298, and 308 K with HAPA concentration of 5.0 mg/L. The thermodynamic parameters, such as the free energy change (ΔG°), standard molar enthalpy (ΔH°), and standard entropy change (ΔS°) were calculated by the following equations [49]:

$$\Delta G^\circ = -RT \ln K_c \tag{10}$$

$$K_c = \frac{C_s}{C_e} \tag{11}$$

$$\ln K_c = \frac{\Delta S^\circ}{R} - \frac{\Delta H^\circ}{RT} \tag{12}$$

in which K_c is equilibrium constant, C_s is the adsorbed amount of HAPA onto AGS at equilibrium state (mg/g), and C_e is the equilibrium concentration of HAPA in the solution.

The values of ΔH° and ΔS° were calculated from the slopes and intercepts of the plots as $\ln K_c$ vs. $1/T$, as shown in Fig. 11. According to Eq. (10), ΔG° was obtained and listed in Table 4. The negative value of ΔG° demonstrated the spontaneous nature of the adsorption, and the decrease with the increasing temperature suggested that higher temperature made the HAPA adsorption much easier onto AGS. The positive value of ΔH° indicated that the adsorption of HAPA onto AGS was endothermic. According to the positive values of ΔS°, the randomness increased at the solid–solution interface with increasing temperature. Similar results were found for the adsorption of acidic dye onto poly grafted AGS [20].

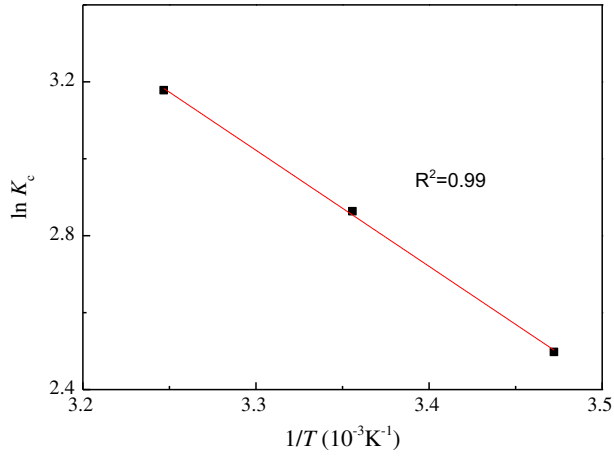

Fig. 11. Plot of $\ln K_c$ vs. $1/T$ (10^{-3} K^{-1}) for the adsorption of HAPA onto AGS.

3.6. Generation of inorganic arsenic

AGS are formed by hundreds and thousands of organisms, which might lead to the degradation of HAPA. Therefore, the generation of inorganic arsenic during the adsorption was measured at the tests without AGS addition and with AGS addition with initial HAPA concentration of 5.0 mg/L. As shown in Fig. 12, 45 μg/L inorganic arsenic without AGS addition and 40 μg/L with AGS addition were detected in the solution at the starting point, which was probably caused by the impurity of the HAPA. In the test with AGS addition, the concentration of inorganic arsenic

Table 4
Thermodynamic parameters for adsorption of HAPA onto AGS

T (K)	ln K_c	ΔG° (kJ/mol)	ΔH° (kJ/mol)	ΔS° (J/(K mol))
288	2.50	−5.98	25.08	107.92
298	2.86	−7.09		
308	3.18	−8.14		

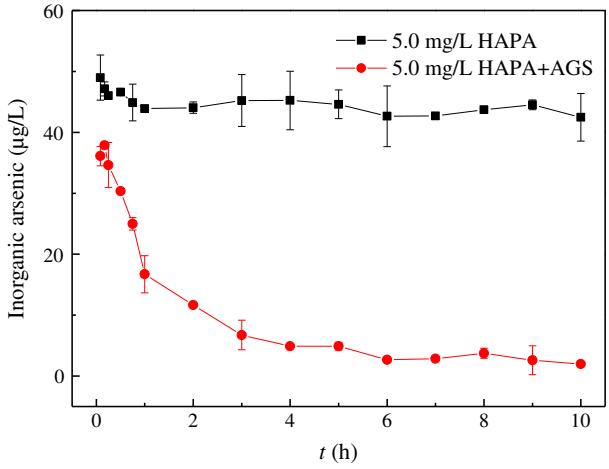

Fig. 12. Inorganic arsenic concentration in the adsorption process.

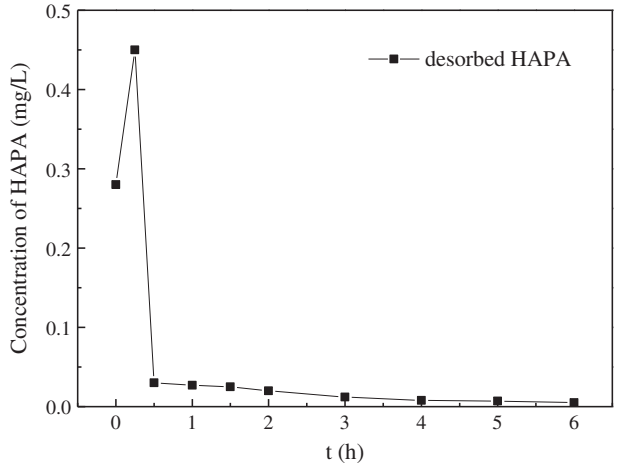

Fig. 13. Desorption curve from AGS after 10-h adsorption of 5 mg/L HAPA.

decreased obviously with the adsorption processing, meaning that inorganic arsenic could also be effectively absorbed by the AGS. The results indicated that the degradation of HAPA by AGS could be neglected in the adsorption experiment.

3.7. Desorption

Fig. 13 shows the concentration of HAPA in the effluent during desorption. The desorption of HAPA from AGS occurred quickly in the first 0.5 h, and completed within 6 h. Only 12% of the absorbed HAPA was washed away during the desorption process, indicating that the adsorption binding between HAPA and AGS was strong in aqueous solution. The results showed that it should be careful to depose of the AGS that was used to treat wastewater containing HAPA for avoiding arsenic contamination.

3.8. Environmental significance

This study demonstrated the adsorption characteristics of AGS toward HAPA, which may be helpful to understand the behavior of HAPA in anaerobic system treating wastewater containing HAPA. It has been reported that HAPA can undergo further decomposition to form arsenite and arsenate, which is highly toxic and bring a risk to the lives in the aquatic environment [50]. Due to the use of roxarsone in animal husbandry, the wastewater containing HAPA would be treated using anaerobic digestion system. The understanding of the adsorption behavior in anaerobic system will improve the management and removal of HAPA and its degradation products from wastewater.

4. Conclusions

The adsorption characteristics of HAPA onto AGS were investigated using batch adsorption experiments in this study. The results showed that the equilibrium state of the adsorption was reached at about 10 h. The maximum adsorption capacity of HAPA onto AGS was 12.57, 25.05, and 26.31 mg/g at 15, 25, and 35°C, respectively. Freundlich and D–R isotherm models fitted the adsorption data very well, and the adsorption was mainly a physical process. The adsorption process followed a pseudo-second-order model and the adsorption binding between HAPA and AGS was

strong in aqueous solution. Intra-particle diffusion was the rate-limiting step for the adsorption of HAPA onto AGS. The increase in pH and phosphate ions had a negative effect on the HAPA adsorption onto AGS. Thermodynamics analysis showed that the adsorption of HAPA onto AGS was an endothermic and spontaneous process. The results obtained from this study will improve the understanding for the fate of roxarsone in anaerobic sludge reactor.

Acknowledgments

This research was partly supported by the NSFC (51578205, 51108149, 51208164), the Science and Technology Innovation Fund from Beijing Academy of Agriculture and Forestry Sciences (CXJJ201317), and the Program for Cultivating Excellent Talents in Beijing (2013D002020000001).

References

[1] A.K. Sarmah, M.T. Meyer, A.B.A. Boxall, A global perspective on the use, sales, exposure pathways, occurrence, fate and effects of veterinary antibiotics (VAs) in the environment, Chemosphere 65 (2006) 725–759.
[2] P. Basu, R.N. Ghosh, L.E. Grove, L. Klei, A. Barchowsky, Angiogenic potential of 3-nitro-4-hydroxy benzene arsonic acid (roxarsone), Environ. Health Perspect. 116 (2008) 520–523.
[3] W.L. Shelver, Generation of antibody and development of an enzyme-linked immunosorbant assay for the feed additive roxarsone, Food Agric. Immunol. 22 (2011) 171–184.
[4] K.P. Mangalgiri, A. Adak, L. Blaney, Organoarsenicals in poultry litter: Detection, fate, and toxicity, Environ. Int. 75 (2015) 68–80.
[5] I. Cortinas, J.A. Field, M. Kopplin, J.R. Garbarino, A.J. Gandolfi, R. Sierra-Alvarez, Anaerobic biotransformation of roxarsone and related N-substituted phenylarsonic acids, Environ. Sci. Technol. 40 (2006) 2951–2957.
[6] J.F. Stolz, E. Perera, B. Kilonzo, B. Kail, B. Crable, E. Fisher, M. Ranganathan, L. Wormer, P. Basu, Biotransformation of 3-nitro-4-hydroxybenzene arsonic acid (roxarsone) and release of inorganic arsenic by *Clostridium* species, Environ. Sci. Technol. 41 (2007) 818–823.
[7] R. Wershaw, Mass spectrometric identification of an azobenzene derivative produced by smectite-catalyzed conversion of 3-amino-4-hydroxyphenylarsonic acid, Talanta 59 (2003) 1219–1226.
[8] R. Sierra-Alvarez, I. Cortinas, J.A. Field, Methanogenic inhibition by roxarsone (4-hydroxy-3-nitrophenylarsonic acid) and related aromatic arsenic compounds, J. Hazard. Mater. 175 (2010) 352–358.
[9] B.P. Jackson, P.M. Bertsch, M.L. Cabrera, J.J. Camberato, J.C. Seaman, C.W. Wood, Trace element speciation in poultry litter, J. Environ. Qual. 32 (2003) 535–540.
[10] L. Shi, W. Wang, S.J. Yuan, Z.H. Hu, Electrochemical stimulation of microbial roxarsone degradation under anaerobic conditions, Environ. Sci. Technol. 48 (2014) 7951–7958.
[11] F.F. Zhang, W. Wang, S.J. Yuan, Z.H. Hu, Biodegradation and speciation of roxarsone in an anaerobic granular sludge system and its impacts, J. Hazard. Mater. 279 (2014) 562–568.
[12] J. Ramaswamy, S.O. Prasher, R.M. Patel, S.A. Hussain, S.F. Barrington, The effect of composting on the degradation of a veterinary pharmaceutical, Bioresour. Technol. 101 (2010) 2294–2299.
[13] W.W. Li, H.Q. Yu, From wastewater to bioenergy and biochemicals via two-stage bioconversion processes: A future paradigm, Biotechnol. Adv. 29 (2011) 972–982.
[14] Y. Mu, X.J. Zheng, H.Q. Yu, R.F. Zhu, Biological hydrogen production by anaerobic sludge at various temperatures, Int. J. Hydrogen Energy 31 (2006) 780–785.
[15] H.Q. Yu, H.H.P. Fang, Acidogenesis of gelatin-rich wastewater in an upflow anaerobic reactor: Influence of pH and temperature, Water Res. 37 (2003) 55–66.
[16] L.W. Hulshoff Pol, S.I. de Castro Lopes, G. Lettinga, P.N. Lens, Anaerobic sludge granulation, Water Res. 38 (2004) 1376–1389.
[17] A.H. Hawari, C.N. Mulligan, Biosorption of lead(II), cadmium(II), copper(II) and nickel(II) by anaerobic granular biomass, Bioresour. Technol. 97 (2006) 692–700.
[18] K. Li, F. Ji, Y.L. Liu, Z.L. Tong, Z. Xinmin, Z.H. Hu, Adsorption removal of tetracycline from aqueous solution by anaerobic granular sludge: Equilibrium and kinetic studies, Water Sci. Technol. 67 (2013) 1490–1496.
[19] J. Bartacek, F.G. Fermoso, A.B. Catena, P.N.L. Lens, Effect of sorption kinetics on nickel toxicity in methanogenic granular sludge, J. Hazard. Mater. 180 (2010) 289–296.
[20] X.F. Sun, S.G. Wang, W. Cheng, M. Fan, B.H. Tian, B.Y. Gao, X.M. Li, Enhancement of acidic dye biosorption capacity on poly(ethylenimine) grafted anaerobic granular sludge, J. Hazard. Mater. 189 (2011) 27–33.
[21] N. Yee, L.G. Benning, V.R. Phoenix, F.G. Ferris, Characterization of metal-cyanobacteria sorption reactions: A combined macroscopic and infrared spectroscopic investigation, Environ. Sci. Technol. 38 (2004) 775–782.
[22] B.H. Hameed, A.A. Ahmad, Batch adsorption of methylene blue from aqueous solution by garlic peel, an agricultural waste biomass, J. Hazard. Mater. 164 (2009) 870–875.
[23] R. Elangovan, L. Philip, K. Chandraraj, Biosorption of chromium species by aquatic weeds: Kinetics and mechanism studies, J. Hazard. Mater. 152 (2008) 100–112.
[24] M.R. Chowdhury, C.N. Mulligan, Biosorption of arsenic from contaminated water by anaerobic biomass, J. Hazard. Mater. 190 (2011) 486–492.
[25] Z.H. Hu, H. Chen, F. Ji, S.J. Yuan, Removal of Congo Red from aqueous solution by cattail root, J. Hazard. Mater. 173 (2010) 292–297.
[26] S. Chowdhury, P. Saha, Sea shell powder as a new adsorbent to remove Basic Green 4 (Malachite Green) from aqueous solutions: Equilibrium, kinetic and thermodynamic studies, Chem. Eng. J. 164 (2010) 168–177.
[27] C.J. An, G.H. Huang, J. Wei, H. Yu, Effect of short-chain organic acids on the enhanced desorption

of phenanthrene by rhamnolipid biosurfactant in soil-water environment, Water Res. 45 (2011) 5501–5510.
[28] X. Wang, S. Xia, J. Zhao, Biosorption of Direct Black 38 by dried anaerobic granular sludge, Front. Environ. Sci. Eng. China 2 (2008) 198–202.
[29] R. Gao, J. Wang, Effects of pH and temperature on isotherm parameters of chlorophenols biosorption to anaerobic granular sludge, J. Hazard. Mater. 145 (2007) 398–403.
[30] Z. Aksu, F. Gönen, Biosorption of phenol by immobilized activated sludge in a continuous packed bed: Prediction of breakthrough curves, Process Biochem. 39 (2004) 599–613.
[31] J. Hu, Z. Tong, Z. Hu, G. Chen, T. Chen, Adsorption of roxarsone from aqueous solution by multi-walled carbon nanotubes, J. Colloid Interface Sci. 377 (2012) 355–361.
[32] V.K. Sharma, M. Sohn, Aquatic arsenic: Toxicity, speciation, transformations, and remediation, Environ. Int. 35 (2009) 743–759.
[33] H. Chiew, M.L. Sampson, S. Huch, S. Ken, B.C. Bostick, Effect of groundwater iron and phosphate on the efficacy of arsenic removal by iron-amended BioSand filters, Environ. Sci. Technol. 43 (2009) 6295–6300.
[34] L.E. Williams, M.O. Barnett, T.A. Kramer, J.G. Melville, Adsorption and transport of arsenic(V) in experimental subsurface systems, J. Environ. Qual. 32 (2003) 841–850.
[35] S. Dixit, J.G. Hering, Comparison of arsenic(V) and arsenic(III) sorption onto iron oxide minerals: Implications for arsenic mobility, Environ. Sci. Technol. 37 (2003) 4182–4189.
[36] A.L. Za, M. Naushad, R. Ali, Kinetic, equilibrium isotherm and thermodynamic studies of Cr(VI) adsorption onto low-cost adsorbent developed from peanut shell activated with phosphoric acid, Environ. Sci. Pollut. Res. 20 (2013) 3351–3365.
[37] J. Zhang, H. Xiao, Y. Zhao, Hemicellulose-based absorbent toward dye: Adsorption equilibrium and kinetics studies, J. Environ. Inform. 24 (2014) 32–38.
[38] L.Z. Miao, C. Wang, J. Hou, P.F. Wang, J. Qian, S.S. Dai, Kinetics and equilibrium biosorption of nano-ZnO Particles on periphytic biofilm under different environmental conditions, J. Environ. Inform. 23 (2014) 1–9.
[39] G.P. Sheng, M.L. Zhang, H.Q. Yu, Characterization of adsorption properties of extracellular polymeric substances (EPS) extracted from sludge, Colloids Surf., B 62 (2008) 83–90.
[40] J.P. Bassin, M. Pronk, R. Kraan, R. Kleerebezem, M.C. van Loosdrecht, Ammonium adsorption in aerobic granular sludge, activated sludge and anammox granules, Water Res. 45 (2011) 5257–5265.
[41] K.V. Kumar, V. Ramamurthi, S. Sivanesan, Modeling the mechanism involved during the sorption of methylene blue onto fly ash, J. Colloid Interface Sci. 284 (2005) 14–21.
[42] Y.J. Shi, X.H. Wang, Z. Qi, M.H. Diao, M.M. Gao, S.F. Xing, S.G. Wang, X.C. Zhao, Sorption and biodegradation of tetracycline by nitrifying granules and the toxicity of tetracycline on granules, J. Hazard. Mater. 191 (2011) 103–109.
[43] W. Ma, X. Song, Y. Pan, Z. Cheng, G. Xin, B. Wang, X. Wang, Adsorption behavior of crystal violet onto opal and reuse feasibility of opal-dye sludge for binding heavy metals from aqueous solutions, Chem. Eng. J. 193–194 (2012) 381–390.
[44] V. Vadivelan, K.V. Kumar, Equilibrium, kinetics, mechanism, and process design for the sorption of methylene blue onto rice husk, J. Colloid Interface Sci. 286 (2005) 90–100.
[45] A. Özcan, E.M. Öncü, A.S. Özcan, Kinetics, isotherm and thermodynamic studies of adsorption of Acid Blue 193 from aqueous solutions onto natural sepiolite, Colloids Surf., A 277 (2006) 90–97.
[46] G. Limousin, J.P. Gaudet, L. Charlet, S. Szenknect, V. Barthès, M. Krimissa, Sorption isotherms: A review on physical bases, modeling and measurement, Appl. Geochem. 22 (2007) 249–275.
[47] J. López-Morales, O. Perales-Pérez, F. Román-Velázquez, Sorption of triclosan onto tyre crumb rubber, Adsorpt. Sci. Technol. 30 (2012) 831–845.
[48] M. Hamayun, T. Mahmood, A. Naeem, M. Muska, S.U. Din, M. Waseem, Equilibrium and kinetics studies of arsenate adsorption by FePO(4), Chemosphere 99 (2014) 207–215.
[49] S. Zhao, G. Huang, C.J. An, J. Wei, Y. Yao, Enhancement of soil retention for phenanthrene in binary cationic gemini and nonionic surfactant mixtures: Characterizing two-step adsorption and partition processes through experimental and modeling approaches, J. Hazard. Mater. 286 (2015) 144–151.
[50] R. Sierra-Alvarez, I. Cortinas, U. Yenal, J.A. Field, Methanogenic inhibition by arsenic compounds, Appl. Environ. Microbiol. 70 (2004) 5688–5691.